

MRI Image Analysis for Alzheimer's Disease Detection Using Transfer Learning: VGGNet vs. EfficientNet

Green Arther Sandag¹, Eleonora Djama², George Morris William Tangka³, Semmy Wellem Taju⁴

^{1,2,3,4}Faculty of Computer Science, Informatics, Universitas Klabat

e-mail: *¹greensandag@unklab.ac.id, ²s2200184@student.unklab.ac.id, ³gtangka@unklab.ac.id, ⁴semmy@unklab.ac.id

Abstract

This study focuses on developing an effective Alzheimer's disease (AD) classification model using MRI images and transfer learning. This research targets individuals aged 65 and above who are affected by the predominant form of dementia and utilizes an Alzheimer's Disease MRI Image dataset from Kaggle. Model selection involved options like EfficientNetB1, B3, B5, B7, VGG16, and VGG19. Two scenarios with distinct batch sizes (10 and 20) were explored in the model creation process. Evaluation, using a confusion matrix, determined that the EfficientNetB5 model yielded the highest accuracy at 99.22%, surpassing other models such as EfficientNetB1, B3, B7, VGG16, and VGG19. Notably, this research highlights the superior performance of EfficientNet over VGGNet in transfer learning for analyzing Alzheimer's disease MRI images. The study concludes with the implementation of a simple web system for testing model outcomes. Overall, the investigation underscores the efficacy of Convolutional Neural Network (CNN) modeling in Alzheimer's disease analysis and identifies EfficientNetB5 as the optimal model for accurate classification.

Keywords— Alzheimer's, Transfer Learning, Deep Learning, VGG, EfficientNet

1. INTRODUCTION

Alzheimer's disease, affecting millions globally, is expected to increase with aging populations. It has profound effects on individuals, families, caregivers, and society. While the exact cause is not fully understood, there is no definitive cure, and existing medications aim to slow progression rather than halt degeneration[1]. According to the 2016 Alzheimer's Disease International (ADI) report, Indonesia had around 1.2 million people diagnosed with dementia. This ranked Indonesia among the top ten countries globally and in Southeast Asia for the highest dementia prevalence in 2015[2]. Projections indicate a rise to 2 million Alzheimer's cases by 2030 and 4 million by 2050. Magnetic Resonance Imaging (MRI) is used to study Alzheimer's-related brain changes. Machine Learning and Deep Learning, applied to neuroimaging data, show promise in predicting and diagnosing AD[3]. Recognizable changes in brain volume, ventricular enlargement, and shifts in MRI signal characteristics can offer insights into the root cause of cognitive decline, commonly referred to as dementia[4]. Technological advances, especially in deep learning for object classification, involve a stepwise transformation and learning process. In image processing, the initial pixel matrix undergoes abstraction, edge encoding, and feature composition, enabling the deep learning model to capture essential characteristics and features efficiently[3]. Recently, advanced deep learning, a subset of machine learning, has focused on acquiring meaningful representations from data through iterative layers, without necessarily implying a deeper understanding. Methods such as Convolutional Neural Networks (CNNs) and sparse autoencoders have outperformed traditional statistical approaches. However, these deep learning methods still face limitations when training deep architectures from scratch[5], [6]. To address limitations, Transfer Learning is introduced, leveraging insights from a larger dataset to enhance the learning process on a smaller target dataset. This proves valuable when training a

classifier solely on a restricted dataset is challenging, showing promising results in EEG-based brain-computer interfaces[7]. Transfer learning improves the initial, accelerates the learning process, and enhances the final performance in a target task by leveraging transferred knowledge[8].

In a related study, Acharya et al[9] employed advanced deep learning methods, including convolutional neural network (CNN) and transfer learning, for accurate Alzheimer's Disease image classification. Transfer learning utilized features from the well-known AlexNet architecture. The proposed approach was evaluated using the Oasis dataset, showcasing a classification rate of 92.86%. Hon et al[10] addressed challenges in Alzheimer's Disease (AD) identification from neuroimaging data, specifically MRI scans, by employing machine learning techniques. They utilized transfer learning, initializing advanced architectures like VGG16 and Inception V4 with pre-trained weights from large-scale benchmark datasets of natural images to overcome these challenges. The accuracy of VGG16 started at 74.12% from scratch but significantly increased to 92.30% with transfer learning. Inception V4 showed an even higher accuracy of 96.25% using the pre-trained model for transfer learning. Ebrahimi et al[11] aimed to detect Alzheimer's Disease (AD) using the ResNet-18 model with Magnetic Resonance Imaging (MRI) data. They innovatively integrated transfer learning into 3D Convolutional Neural Networks (CNNs), enabling knowledge transfer from 2D to 3D image datasets. Through optimization during training, their method achieved an accuracy of 96.88%, 100% sensitivity, and 93.75% specificity.

This study examines the accuracy levels obtained from selected model architectures with the potential to classify Alzheimer's Disease MRI images into 4 classes: 'NonDemented', 'MildDemented', 'VeryMildDemented', 'ModerateDemented'. The models tested include EfficientNetB1, EfficientNetB3, EfficientNetB5, EfficientNetB7, VGG16, and VGG19, using the Alzheimer's Disease MRI Image dataset from Kaggle. The model with the highest accuracy will be chosen for implementation in a simple web system designed to showcase the testing results of Alzheimer's Disease MRI images.

2. RESEARCH METHODS

In Figure 1 data is collected using an Alzheimer's Disease MRI Image dataset from Kaggle. Models such as EfficientNetB1, B3, B5, B7, VGG16, and VGG19 are considered for transfer learning or modifications. The process includes data preprocessing with various feature extraction techniques, feature extraction is vital in applications like diagnosis, classification, clustering, recognition, and detection, especially in image processing tasks[12], followed by modeling using CNN architectures (EfficientNet and VGGNet) to classify MRI images into four classes. Evaluation involves a confusion matrix to assess accuracy, recall, precision, and F1-score. A comparative analysis among the six models helps identify the most optimal one based on accuracy. The chosen model is then integrated into a user-friendly web application. Before deployment, thorough testing is conducted to address potential errors. The web system allows users to upload an MRI image, classifying it into four classes and displaying the image with the corresponding percentage.

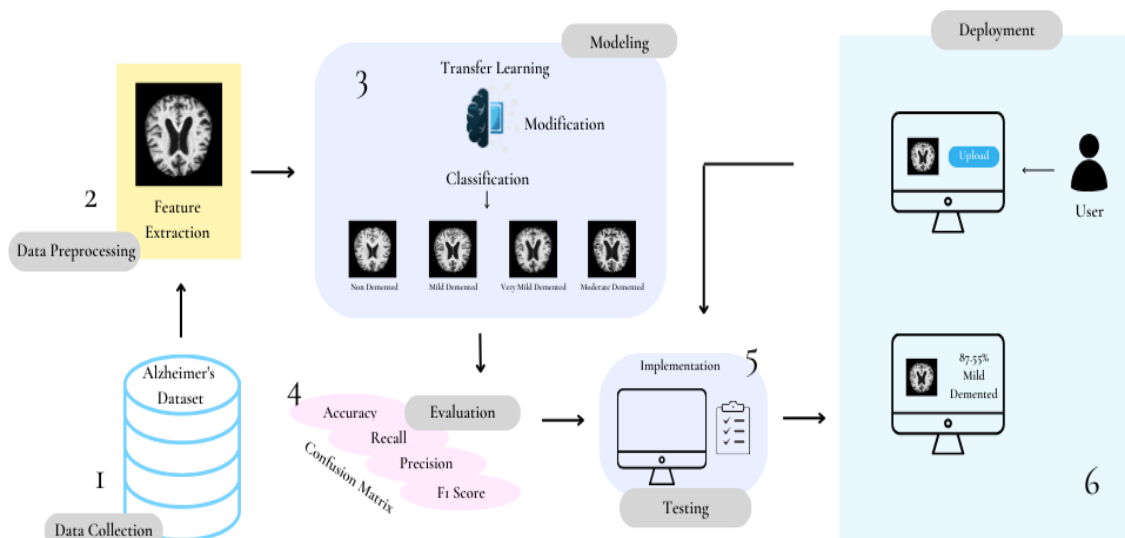


Figure 1. Research Design Methodology Framework

2.1 Data Collection

We utilized an Alzheimer's dataset obtained from Kaggle, consisting of four distinct image classes. The dataset includes a total of 5,120 MRI images, distributed as follows: 2,560 non-demented individuals, 1,792 individuals with very mild dementia, 717 individuals with mild dementia, and 51 individuals with moderate dementia. Due to the scarcity of images for the moderate dementia category, we decided to augment the dataset by adding 149 images specifically for this classification. Consequently, the dataset now consists of 5,269 MRI images.

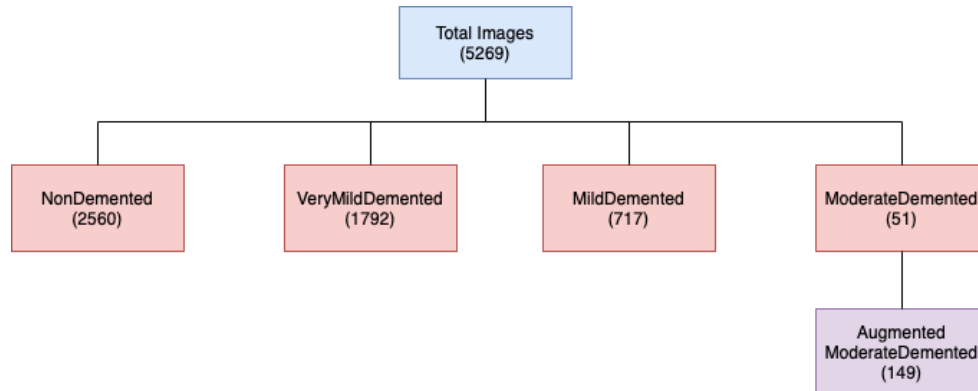


Figure 2. Total MRI Images in Dataset

2.2 Data Preprocessing

In this research phase, data augmentation plays a vital role in enhancing dataset quality. Utilizing Keras' ImageDataGenerator, the process aims to expand the dataset by introducing significant variations through various transformations. The code identifies classes with insufficient samples, calculates the required additional images, and uses the ImageDataGenerator to create and save augmented images in corresponding class subdirectories. This approach enhances dataset diversity and ensures a balanced class distribution, promoting the training of robust machine learning models.

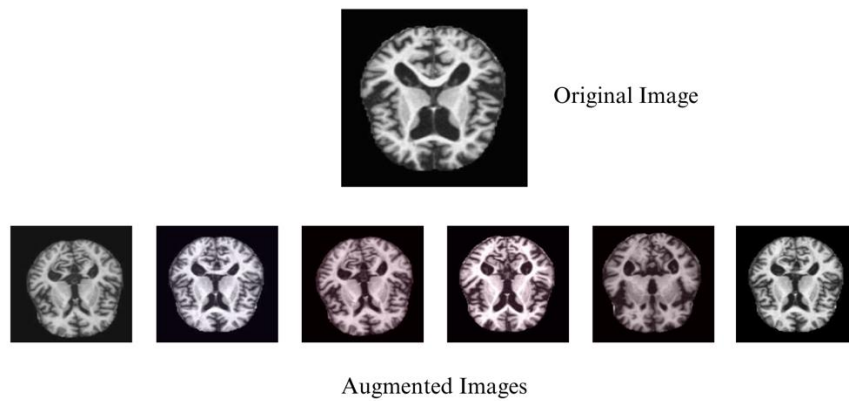


Figure 3. Augmented Images Samples

Figure 3 visually illustrates the augmentation process, elucidating the transformations applied to the dataset. This involves a sequence of image manipulations such as horizontal flipping, rotation (up to 20 degrees), adjustments in width and height (up to 20%), zooming (up to 20%), shearing (up to 20%), brightness modification (ranging from 0.8 to 1.2 times), color manipulation (red or green), and channel shifting (up to 10.0). These transformations play a crucial role in enhancing dataset variability, thereby aiding machine learning models in effective generalization. In addition to augmentation, image normalization is applied to ensure consistency across input data. Each pixel value in the images is rescaled to a range of [0,1] by dividing all pixel values by 255. This transformation standardizes input values, reducing computational complexity and stabilizing model convergence.

2.3 Modeling

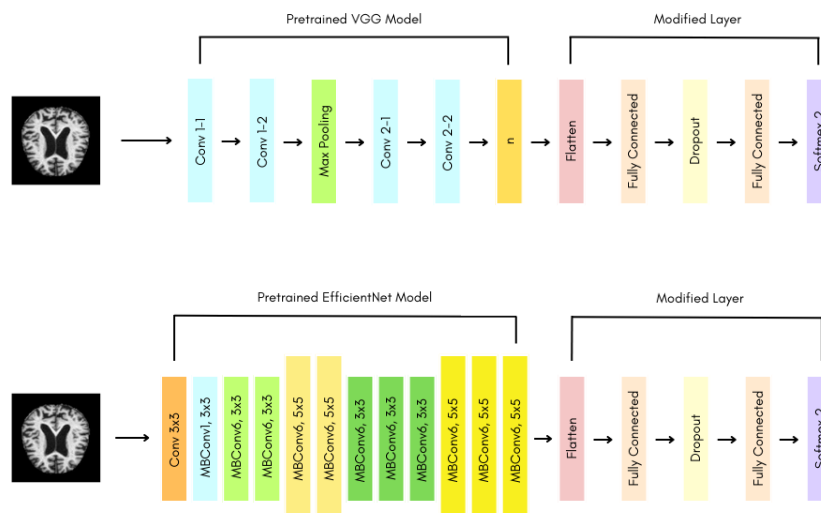


Figure 4. Modified Layer

In the next stage, the deep learning process is conducted using the CNN technique, focusing on transfer learning with EfficientNet and VGGNet. The selection of these models is based on their proven effectiveness in medical image classification, as demonstrated in previous studies[13,14,15]. EfficientNet introduces an innovative scaling approach that optimizes neural network performance by uniformly adjusting depth, width, and resolution using a compound coefficient. This model has shown superior accuracy and efficiency in various image classification tasks, including medical imaging. VGGNet, specifically VGG16, and VGG19, is widely recognized for its deep architecture, which expands the receptive field using small

convolutional kernels while maintaining a straightforward structure[16,17,18]. Its hierarchical feature extraction capability makes it a strong candidate for analyzing medical images, including MRI scans. In this study, both EfficientNet and VGGNet architectures are customized by preserving the Convolution and Max Pooling layers while modifying the Flatten, Fully Connected, and Dropout layers. These modifications are designed to optimize classification performance and produce a softmax output with four categories: Mild Dementia, Very Mild Dementia, Moderate Dementia, and Non-Dementia.

Table 1. Parameters

Scenario	Optimizer	Epoch	LR	Loss Function	Batch Size
1	Adamax, SGD, dan RMSProp	30	0.001	Categorical	10
2	Adamax, SGD, dan RMSProp	30	0.001	Categorical	20

The next step involved experimenting with modeling by employing transfer learning techniques with VGG16, VGG19, EfficientNetB1, EfficientNetB3, EfficientNetB5, and EfficientNetB7. The model creation process consisted of two scenarios, each defined by its batch size: Scenario 1 with a batch size of 10 and Scenario 2 with a batch size of 20. These batch sizes were selected based on findings from previous studies [3,11,16], which suggest that smaller batch sizes (e.g., 10–32) can improve generalization in medical image classification tasks by preventing overfitting and enhancing convergence stability. Additionally, due to hardware constraints and memory limitations in training deep learning models with high-resolution MRI images, these batch sizes were chosen to maintain computational efficiency while ensuring model performance.

These scenarios incorporated variations using different optimizers, namely Adamax, SGD, and RMSProp, all utilizing the Categorical Crossentropy loss function. Future work could further explore the impact of different batch sizes on model performance to optimize training stability and classification accuracy.

2.4 Evaluation

During this phase, we assess image classification results using a confusion matrix. The objective is to determine the accuracy, precision, recall, and F1-score of the employed dataset. The formula is provided below:

$$Accuracy = \frac{TP+TN}{TP+FP+FN+TN} \quad (1)$$

$$Precision = \frac{TP}{FP+TP} \quad (2)$$

$$Recall = \frac{TP}{TP+FN} \quad (3)$$

$$F1-Score = \frac{2 \times Recall \times Precision}{Recall+Precision} \quad (4)$$

We also assess the loss and accuracy graphs of the machine learning model for performance evaluation. These visual indicators track the model's learning progress, with the loss graph depicting predictive errors and guiding adjustments, while the accuracy graph reflects the overall correctness of predictions. Examining these graphs provides a nuanced understanding of the model's adaptation and learning from the training data.

2.5 Deployment

In the concluding phase, we create a straightforward web system for categorizing Alzheimer's disease images. The system is tailored to precisely recognize Alzheimer's disease and

assign appropriate classifications. The results will display the class of the Alzheimer’s Disease MRI scan and the corresponding accuracy percentage.

3. RESULTS AND DISCUSSION

3.1 Comparative analysis of the best transfer learning model in two different scenarios

Table 2. Comparative of the Best Performing Transfer Learning Models (VGG16, VGG19, EfficientNetB1, B3, B5, and B7)

Model	Optimizer	Loss Function	Accuracy	Scenario
VGG16	SGD	Categorical	76.41%	1
VGG19	SGD	Categorical	80.78%	1
EfficientNetB1	Adamax	Categorical	95.78%	1
EfficientNetB3	Adamax	Categorical	93.28%	2
EfficientNetB5	Adamax	Categorical	99.22%	1
EfficientNetB7	Adamax	Categorical	97.34%	1

Table 2 evaluates the performance of VGG16, VGG19, and various EfficientNet models (B1, B3, B5, and B7) for Alzheimer's disease classification using different optimization strategies and loss functions. VGG16 and VGG19, optimized with Stochastic Gradient Descent (SGD) and categorical cross-entropy loss, achieve accuracies of 76.41% and 80.78% under Scenario 1, respectively. In contrast, EfficientNet models demonstrate superior accuracy, with EfficientNetB1 reaching 95.78%, EfficientNetB5 achieving the highest accuracy of 99.22%, and EfficientNetB7 scoring 97.34%, all using the Adamax optimizer and categorical loss in Scenario 1, while EfficientNetB3 attains 93.28% in Scenario 2. The consistent use of the Adamax optimizer highlights its effectiveness over SGD, offering better convergence and generalization. The scenario-based variation, particularly the reduced accuracy of EfficientNetB3 in Scenario 2, suggests a need for further exploration of data complexity and task-specific conditions. Overall, EfficientNetB5 sets a benchmark in performance, reinforcing the impact of advanced optimizers and architecture choices on classification accuracy.

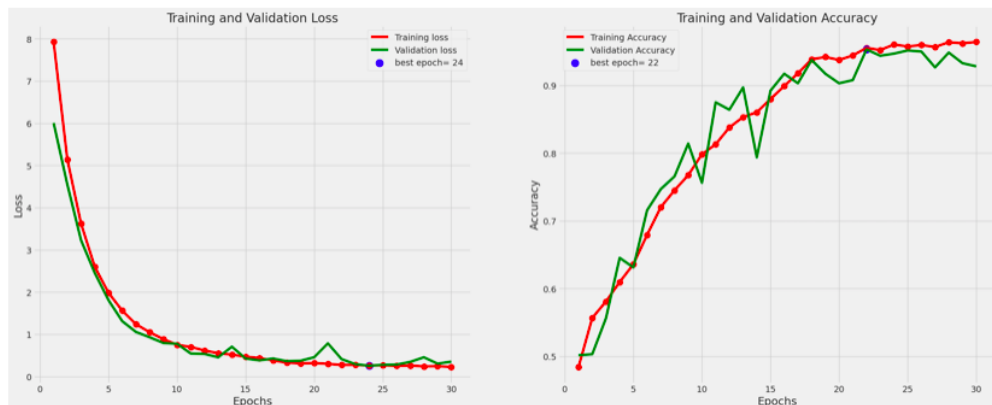


Figure 5. Scenario 1 EfficientNetB5 Loss and Accuracy Graph

Figure 5 illustrates the training and validation loss (left) and accuracy (right) over 30 epochs for the EfficientNetB5 model. The loss graph on the left demonstrates a rapid decrease in both training and validation losses during the early epochs, with both curves converging around epoch 24, which is highlighted as the best epoch for loss. This behavior indicates effective

learning and no significant overfitting throughout training. In the accuracy graph on the right, both training and validation accuracy curves rise steadily, with validation accuracy peaking at epoch 22, designated as the best epoch. The close alignment of these curves suggests good generalization capability, though minor fluctuations in validation accuracy hint at occasional performance variability.

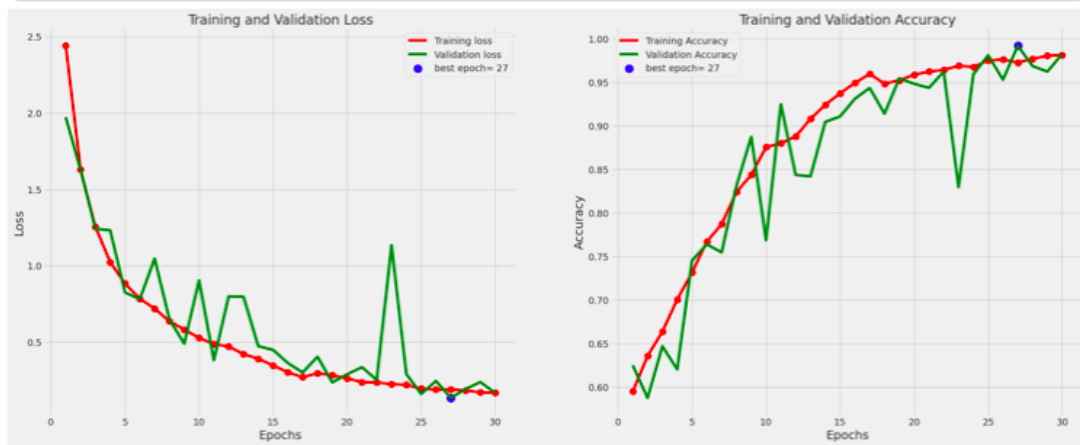


Figure 6. Scenario 2 EfficientNetB7 Loss and Accuracy Graph

Figure 6 depicts the training and validation loss (left) and accuracy (right) over 30 epochs for the EfficientNetB7 model. The loss graph shows that training loss declines consistently, whereas validation loss decreases with noticeable oscillations, stabilizing after epoch 20 and reaching its best point at epoch 27. The accuracy graph on the right displays a smooth increase in training accuracy, while validation accuracy fluctuates more significantly, aligning with training accuracy after epoch 20. The best validation accuracy is recorded at epoch 27, reflecting successful training and generalization. Despite the observed variability in validation metrics, the overall trends confirm the model's strong performance and resilience to overfitting.

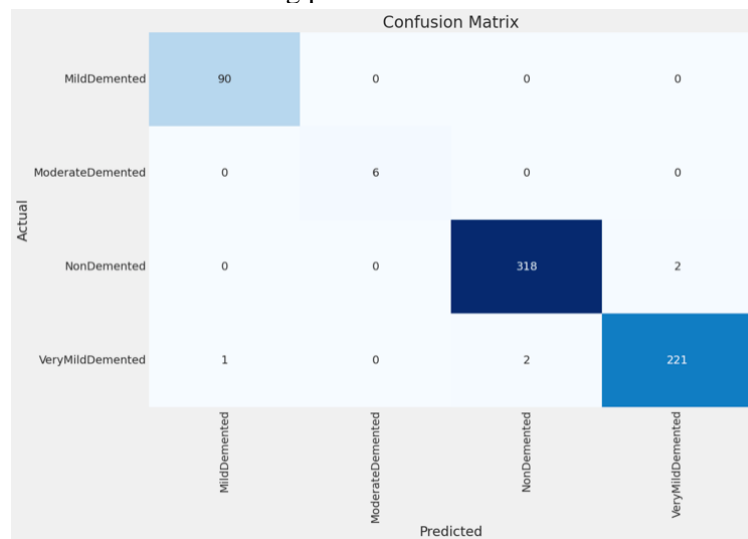


Figure 7. Scenario 1 EfficientNetB5 Confusion Matrix

The confusion matrix above demonstrates that the EfficientNet B5 model in Scenario 1 performs exceptionally well in classifying the NonDemented class (TP: 318, FP: 2), with minimal misclassifications. The MildDemented (TP: 90) and VeryMildDemented (TP: 221) classes also show high performance, with only minor errors (FN: 1 and FN: 2, respectively). For the ModerateDemented class, all predictions are correct (TP: 6), but the small number of samples in

this class may impact evaluation stability. However, some misclassifications are observed, notably VeryMildDemented cases misclassified as NonDemented (2 instances) and MildDemented (1 instance), as well as NonDemented cases, misclassified as VeryMildDemented (2 instances). These errors suggest potential feature overlap between these dementia stages, making differentiation more challenging. Furthermore, the small sample size in the ModerateDemented category may result in an unstable evaluation of model performance.

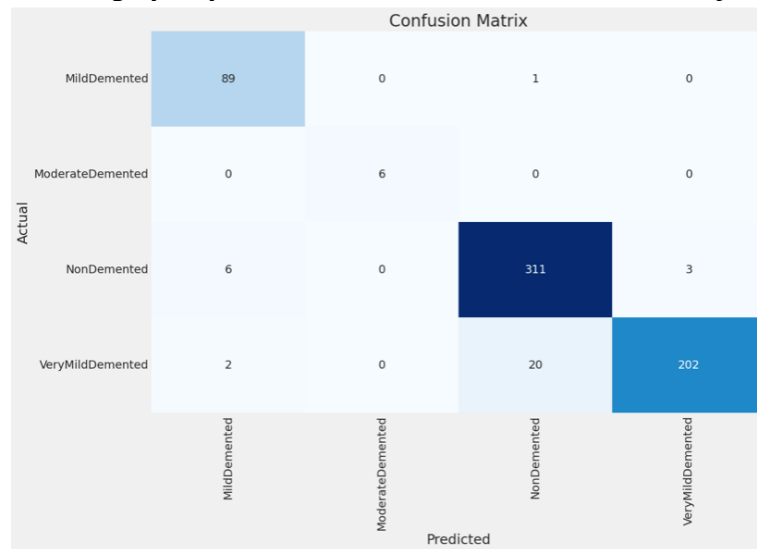


Figure 8. Scenario 2 EfficientNetB7 Confusion Matrix

According to Figure 8, the confusion matrix for the best model in Scenario 2 using EfficientNet B7 demonstrates strong performance across all classes. For MildDemented, the model correctly predicted 89 instances, with minimal errors (1 misclassified as NonDemented and 2 misclassified as VeryMildDemented). The ModerateDemented class achieved perfect classification (6 TP), though the small sample size suggests caution in interpretation. For NonDemented, the model correctly classified 311 cases, but 6 were misclassified as MildDemented and 20 as VeryMildDemented, indicating some difficulty in distinguishing between these stages. Similarly, for VeryMildDemented, the model predicted 202 instances correctly, but 20 were misclassified as NonDemented and 2 as MildDemented, suggesting an overlap in feature representation. These misclassifications between NonDemented and VeryMildDemented indicate that the model struggles to differentiate between early-stage dementia and healthy individuals. Furthermore, it is important to note that this study did not employ k-fold cross-validation. Instead, a train-validation-test split was used to evaluate model performance while ensuring independence between training and testing data. This approach was chosen to better reflect real-world deployment scenarios and prevent potential data leakage. However, we acknowledge the advantages of cross-validation in providing a more robust performance estimate, and future work may explore its implementation to further validate the model’s stability across different data partitions.

3.2 Comparison with Related Research

Table 3. Comparison with Other Related Research

Research Name	Model	Dataset	Best Model Accuracy Result	Classification Method
Acharya et al.[9]	CNN, VGG 16, ResNet and AlexNet	Alzheimer MRI Images Kaggle Dataset	Modified AlexNet (95.70%)	Multiclass
Zaabi et al.[19]	DNN, CAE, Inception, CNN Modified AlexNet	Open Access Series of Imaging Studies (OASIS) Dataset: Cross-sectional MRI Data	Modified AlexNet (92.86%)	Binary
Hon et al.[10]	VGG and Inception	Open Access Series of Imaging Studies (OASIS) Dataset: Cross-sectional MRI Data	Inception V4 (96.25%)	Binary
Abed et al.[20]	VGG19, Inception v3, ResNet50	Alzheimer's Disease Neuroimaging Initiative (ADNI)	VGG19 (98%)	Multiclass
Ebrahimi et al.[11]	2D Resnet-18, 3D Resnet-18, Adjusted 3D ResNet-18	Alzheimer's Disease Neuroimaging Initiative (ADNI)	3D Resnet-18 (96.88%)	Binary
This research	Vgg16, Vgg19, EfficientNetB1, EfficientNetB3, EfficientNetB5, EfficientNet B7	Alzheimer MRI Images Kaggle Dataset	EfficientNetB5 (99.22%)	Multiclass

Table 3 compares the results of various research studies on Alzheimer's disease classification using different models, datasets, and methods. Acharya et al. achieved 95.70% accuracy with a modified AlexNet on the Kaggle Alzheimer MRI dataset for multiclass classification. Zaabi et al. used the OASIS dataset for binary classification and reached 92.86% accuracy with a modified AlexNet. Hon et al. obtained 96.25% accuracy with Inception V4 on the OASIS dataset for binary classification, while Abed et al. achieved 98% accuracy with VGG19 on the ADNI dataset for multiclass classification. Ebrahimi et al. reported 96.88% accuracy using a 3D ResNet-18 on the ADNI dataset for binary classification. In this research, the EfficientNetB5 model achieved the highest accuracy of 99.22% on the Kaggle Alzheimer MRI dataset for multiclass classification, outperforming other studies in both accuracy and multiclass performance. We acknowledge the differences in complexity and challenges between multiclass and binary classification tasks. The inclusion of both types of studies in the comparison was intended to provide a comprehensive perspective on the performance of deep learning models in Alzheimer's disease classification. While binary classification focuses on distinguishing between two categories (e.g., Alzheimer's vs. Non-Alzheimer's), multiclass classification provides a more granular analysis by differentiating between multiple stages of dementia.

Our study primarily focuses on multiclass classification, as it aligns with the goal of early-stage Alzheimer's detection and progression monitoring. However, we included binary classification studies in the comparison to highlight the effectiveness of different deep learning architectures in the domain of Alzheimer's diagnosis, regardless of the classification method used. Additionally, by showcasing the performance of EfficientNetB5 in a multiclass setting, we aim to emphasize its ability to handle increased complexity while achieving superior accuracy.

3.3 Alzheimer's Disease Classification Web System

In the following figure 9 is the completion of model development and evaluation, we implement a basic web system to test the model's outcomes. Users can upload images to the system, and the model will predict and classify them into one of four categories: 'Mild Dementia,' 'Very Mild Dementia,' 'Moderate Dementia,' and 'Non-Dementia.'

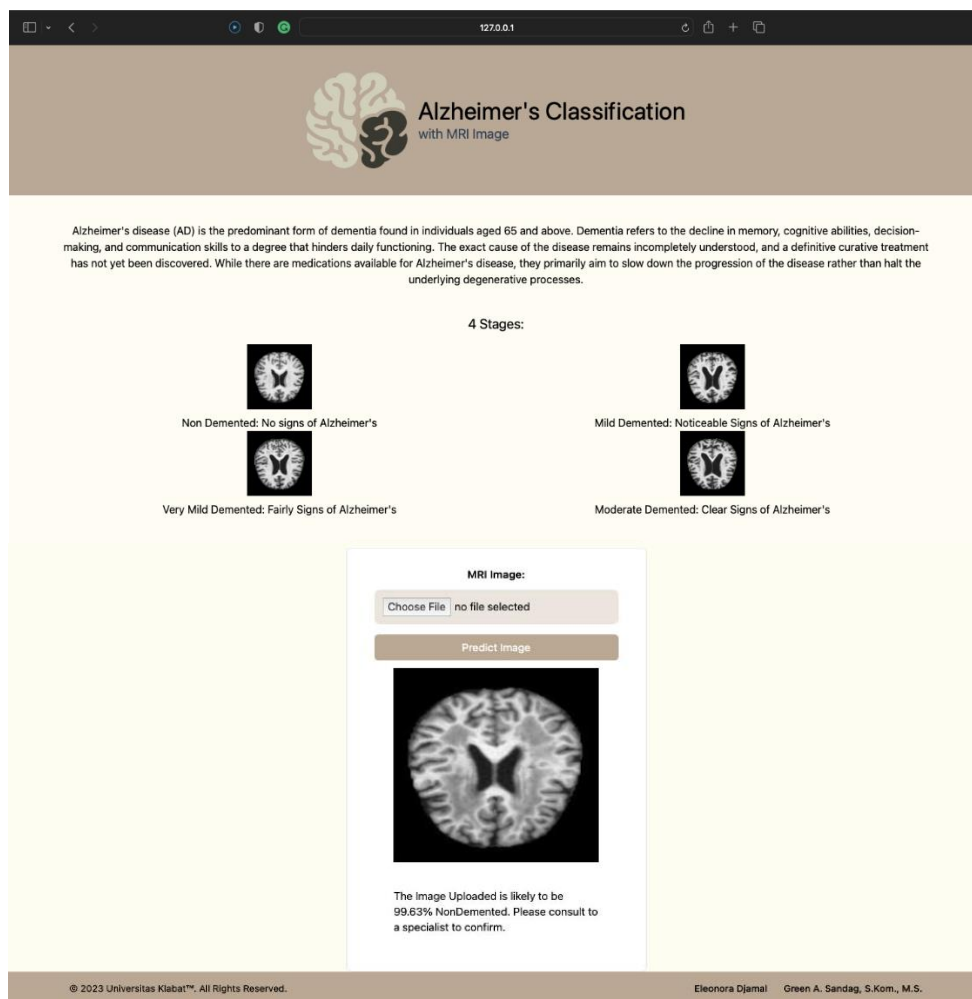


Figure 9. Alzheimer's Disease Classification Website

It demonstrates that after uploading an image, the web system proceeds to analyze the image for predictions. Within the prediction form, there is a section specifically designated to showcase the prediction result. In this specific case, it includes an uploaded image classified as "NonDemented." Consequently, the prediction result will indicate a high probability that the uploaded image is classified as "NonDemented," along with the corresponding likelihood percentage provided in the statement.

4. CONCLUSION

In this study, we employed Convolutional Neural Network (CNN) modeling combined with transfer learning to analyze Alzheimer's disease MRI images, utilizing VGGNet and EfficientNet architectures. Among the tested models, EfficientNetB5 demonstrated the highest performance, achieving an accuracy of 99.22%, outperforming other variants such as EfficientNetB1, B3, and B7, as well as VGG16 and VGG19. These findings indicate the effectiveness of EfficientNet over VGGNet for transfer learning in this domain. Through extensive experiments using a learning rate of 0.001, batch sizes of 10 and 20, and categorical cross-entropy loss, the models consistently delivered strong classification performance. However, it is important to acknowledge that this study did not employ k-fold cross-validation, and further validation using different datasets and evaluation techniques is recommended.

5. FUTURE WORKS

Future research could explore a wider range of transfer learning models, including architectures like ResNet, Inception, DenseNet, and Vision Transformers, to compare their performance with EfficientNet and VGGNet in the classification of Alzheimer's disease MRI images. Such comparative studies would provide a more comprehensive understanding of the strengths and limitations of different models in this context. Additionally, incorporating advanced techniques such as ensemble learning, multi-modal data integration (e.g., combining MRI with genetic or clinical data), and self-supervised learning could further enhance model performance and generalization. Beyond Alzheimer's disease, expanding the scope of image classification to include other neurological disorders such as Parkinson's disease or multiple sclerosis, as well as other medical conditions like cancers, cardiovascular diseases, and diabetic retinopathy, could deliver significant public health benefits. This broader application would facilitate early detection and improve diagnostic accuracy across diverse medical fields. Moreover, addressing challenges such as imbalanced datasets, explainability of AI models, and computational efficiency could strengthen the applicability and trustworthiness of AI in healthcare. Ultimately, these advancements would not only refine the application of AI in medical imaging but also contribute to improving patient outcomes on a global scale.

REFERENCES

- [1] *Alzheimers Disease Current and Future Perspectives*. OMICS International, 2016. doi: 10.4172/978-1-63278-067-6-68.
- [2] S. E. Martina, "Caregiver Training on Care for People With Dementia in Medan, North Sumatera," *Darmabakti Cendekia J. Community Serv. Engag.*, vol. 2, no. 1, p. 1, 2020, doi: 10.20473/dc.v2.i1.2020.1-3.
- [3] M. Leela, K. Helenprabha, and L. Sharmila, "Prediction and classification of Alzheimer Disease categories using Integrated Deep Transfer Learning Approach," *Meas. Sensors*, vol. 27, Jun. 2023, doi: 10.1016/j.measen.2023.100749.
- [4] "World Alzheimer Report 2021: Journey through the diagnosis of dementia."
- [5] N. M. Khan, N. Abraham, and M. Hon, "Transfer Learning with Intelligent Training Data Selection for Prediction of Alzheimer's Disease," *IEEE Access*, vol. 7, pp. 72726–72735, 2019, doi: 10.1109/ACCESS.2019.2920448.
- [6] P. A. Miceli, W. D. Blair, and M. M. Brown, "Isolating random and bias covariances in tracks," in *Proc. 21st Int. Conf. Inf. Fusion (FUSION)*, Cambridge, UK, Jul. 2018, pp. 2437–2444.

-
- [7] S. Sidharth, A. A. Samuel, R. H, J. T. Panachakel, and S. P. K, "Emotion Detection from EEG using Transfer Learning," in 2023 45th Annual International Conference of the IEEE Engineering in Medicine & Biology Society (EMBC), Jul. 2023, pp. 1–4. doi: 10.1109/EMBC40787.2023.10340389.
- [8] R. Gupta, K. K. Bhardwaj, and D. K. Sharma, "Transfer Learning," in *Machine Learning and Big Data*, John Wiley & Sons, Ltd, 2020, pp. 335–360. doi: [10.1002/9781119654834.ch13](https://doi.org/10.1002/9781119654834.ch13).
- [9] H. Acharya, R. Mehta, and D. K. Singh, "Alzheimer disease classification using transfer learning," in *Proc. 5th Int. Conf. Comput. Methodol. Commun. (ICCMC)*, Erode, India, Apr. 2021, pp. 1503–1508, doi: 10.1109/ICCMC51019.2021.9418294.
- [10] M. Hon and N. M. Khan, "Towards Alzheimer's disease classification through transfer learning," in *Proc. IEEE Int. Conf. Bioinf. Biomed. (BIBM)*, Kansas City, MO, USA, Nov. 2017, pp. 1166–1169.
- [11] A. Ebrahimi, S. Luo, and R. Chiong, "Introducing transfer learning to 3D ResNet-18 for Alzheimer's disease detection on MRI images," in *Proc. 35th Int. Conf. Image Vis. Comput. N. Z. (IVCNZ)*, Wellington, New Zealand, Nov. 2020, pp. 1–6. doi: 10.1109/IVCNZ51579.2020.9290616.
- [12] W. K. Mutlag, S. K. Ali, Z. M. Aydam, and B. H. Taher, "Feature extraction methods: a review," in *J. Phys.: Conf. Ser.*, vol. 1591, no. 1, p. 012028, Jul. 2020, IOP Publishing. doi: 10.1088/1742-6596/1591/1/012028.
- [13] A. S. Ebenezer, S. D. Kanmani, M. Sivakumar, and S. J. Priya, "Effect of image transformation on EfficientNet model for COVID-19 CT image classification," *Mater. Today: Proc.*, vol. 51, pp. 2512–2519, 2022, doi: 10.1016/j.matpr.2021.12.121.
- [14] M. Tan and Q. Le, "EfficientNet: Rethinking model scaling for convolutional neural networks," in *Proc. Int. Conf. Mach. Learn.*, Long Beach, CA, USA, May 2019, pp. 6105–6114, PMLR.
- [15] Z. Liu, J. John, and E. Agu, "Diabetic foot ulcer ischemia and infection classification using EfficientNet deep learning models," *IEEE Open J. Eng. Med. Biol.*, vol. 3, pp. 189–201, 2022.
- [16] Z. Cao, J. Huang, X. He, and Z. Zong, "BND-VGG-19: A deep learning algorithm for COVID-19 identification utilizing X-ray images," *Knowledge-Based Syst.*, vol. 258, p. 110040, 2022, doi: 10.1016/j.knosys.2022.110040.
- [17] X. Zhao, L. Wang, Y. Zhang, X. Han, M. Deveci, and M. Parmar, "A review of convolutional neural networks in computer vision," *Artif. Intell. Rev.*, vol. 57, no. 4, p. 99, 2024.
- [18] R. Zhang, P. Isola, A. A. Efros, E. Shechtman, and O. Wang, "The unreasonable effectiveness of deep features as a perceptual metric," in *Proc. IEEE Conf. Comput. Vis. Pattern Recognit. (CVPR)*, Salt Lake City, UT, USA, Jun. 2018, pp. 586–595.
- [19] M. Zaabi, N. Smaoui, H. Derbel, and W. Hariri, "Alzheimer's disease detection using convolutional neural networks and transfer learning based methods," in *Proceedings of the 17th International Multi-Conference on Systems, Signals and Devices, SSD 2020*,
-

Institute of Electrical and Electronics Engineers Inc., Jul. 2020, pp. 939–943. doi: 10.1109/SSD49366.2020.9364155.

- [20] M. T. Abed, U. Fatema, S. A. Nabil, M. A. Alam, and M. T. Reza, "Alzheimer's disease prediction using convolutional neural network models leveraging pre-existing architecture and transfer learning," in *Proc. Joint 9th Int. Conf. Informatics, Electron. & Vis. (ICIEV) and 4th Int. Conf. Imaging, Vis. & Pattern Recognit. (icIVPR)*, Kitakyushu, Japan, Aug. 2020, pp. 1–6. doi: 10.1109/ICIEVicIVPR48672.2020.9306649.